Angewandte Chemie
Eine Zeitschrift der Gesellschaft Deutscher Chemiker

# Supporting Information

© Wiley-VCH 2006

69451 Weinheim, Germany

# Modulation of DNA Constraints that Control Macromolecular Folding

Chandrasekhar V. Miduturu and Scott K. Silverman*

Department of Chemistry, University of Illinois at Urbana-Champaign, 600 South Mathews Avenue, Urbana, IL 61801 (USA)

## Table of Contents

General experimental considerations

Standard DNA oligonucleotides were prepared by solid-phase synthesis at Integrated DNA Technologies (Coralville, IA). DNA oligonucleotides incorporating a 5′-modified phosphoramidite as well as all RNA oligonucleotides were prepared by solid-phase synthesis at the UIUC W. M. Keck Center. Transcription of P4-P6 RNA sequences used T7 RNA polymerase and a linearized plasmid DNA template.[1] The plasmids encoding P4-P6-wt (nt 102-261), P4-P6-bp (nt 102-261 with nt 123-126 ACAG in the J5/5a joining region[2] replaced with UGU), and Δ15-P4-P6 (nt 117-261; fragments **II**+**III** of Figure S2 in both wt and bp versions) were available from a previous study.[1] The plasmid encoding P4-P6 nt 117-237 terminating with a 2′,3′-cyclic phosphate via a co-transcriptional hammerhead ribozyme (fragment **II** of Figure S2 in both wt and bp versions) was prepared by standard PCR and cloning methods from the plasmid encoding P4-P6-24 (nt 102-237 terminating with a cyclic phosphate, in both wt and bp versions).[3] All oligonucleotides, transcripts, and ligation products were purified by denaturing PAGE.[4] The experimental procedure for native PAGE is described in detail in ref. 5. The secondary structure of P4-P6 is shown in Figure S1.

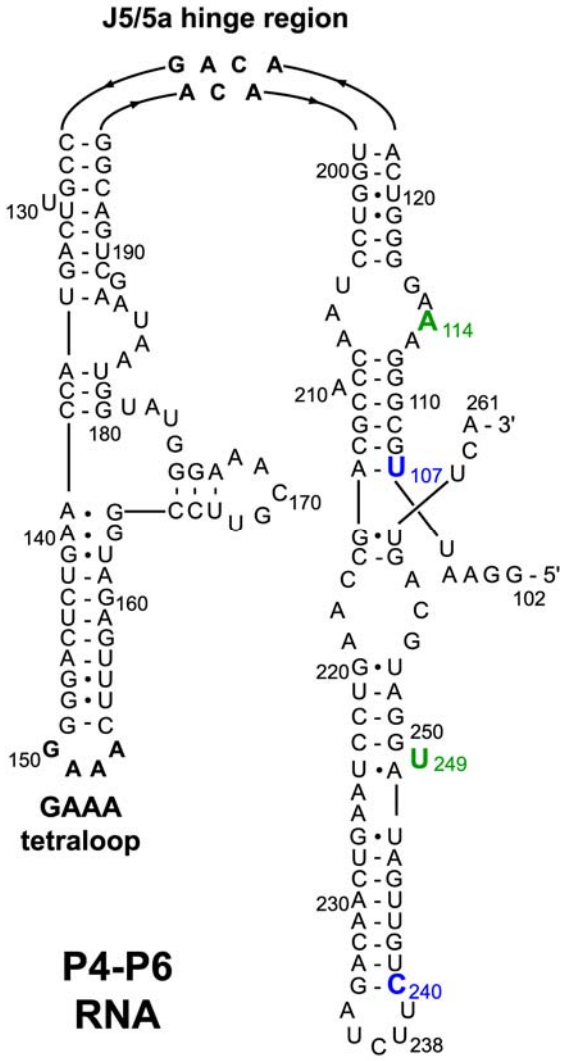


**Figure S1.** Secondary structure of the P4-P6 RNA. The two pairs of nucleotides (U107-C240 and A114-U249) that were separately modified with DNA are highlighted.

Preparation of RNA-DNA conjugates

For synthesis of RNA-DNA conjugates with N-linked constraints, the procedure shown in Figure S2a was used. The detailed experimental steps of this procedure were given in our previous publication that introduced the DNA constraints approach.[5] For RNA-DNA conjugates with one N-linked constraint and one S-linked constraint, the modified procedure shown in Figure S2b was used. All steps of the procedure up to RNA-DNA disulfide formation were performed in the same way as the analogous steps of Figure S2a.

*Formation of 5′-disulfide-DNA.* A portion of *S*-trityl-protected 5′-thiol-DNA (5 nmol, prepared using a modified phosphoramidite that was synthesized as reported[6]) was mixed with $AgNO_3$ (500 nmol) in 30 μL of 50 mM triethylammonium acetate (pH 7.0) and incubated at 37 °C for 3 h. Separately, an 0.5 M solution of phenyl 2-pyridyl disulfide (PhSSPy) was prepared by mixing equal volumes of 1 M PhSH in methanol and 1 M PySSPy in methanol. To the deprotected 5′-thiol-DNA was added 4 μL of the PhSSPy solution and Tris (pH 8.0) to 100 mM. The sample was incubated at room temperature for 16 h. The sample was extracted with ethyl acetate (2 × 75 μL), and the organic extracts were back-extracted with water (25 μL). The combined aqueous extracts were concentrated on a SpeedVac to remove residual ethyl acetate, desalted on a Sephadex G-25 spin column (Amersham), and diluted to 50 μL with water. Quantification by UV absorbance ($A_{260}$) indicated a typical yield of 4.5 nmol of 5′-disulfide-DNA.

*RNA deprotection with $AgNO_3$.* A portion of 5′-$^{32}$P-radiolabeled **I**–**II**–**III** (5 pmol) was mixed with a disruptor DNA oligonucleotide (500 pmol of sequence complementary to P4-P6 nucleotides 175–225) and a 20-nt DNA oligonucleotide complementary to the constraint strand that is attached via reductive amination at U249 (100 pmol) in a total volume of 5 μL containing 5 mM Tris (pH 7.5) and 0.1 mM EDTA. The sample was annealed by heating at 95 °C for 3 min and cooling on ice for 5 min. This sample was mixed with $AgNO_3$ (500 pmol) in a 7.5-μL solution containing 15 mM triethylammonium acetate (pH 7.0). The colorless solution was incubated at 37 °C for 3 h, and 1 μL of 3 M NaCl was added to precipitate the excess $Ag^+$ as AgCl.

*Preparation of RNA-DNA disulfide conjugate.* The 8.5-μL sample of deprotected RNA was added to an evaporated residue of 5′-disulfide-DNA (1 nmol) followed by addition of 1 μL of 1 M Tris (pH 8.0) and 0.5 μL of water. The colorless solution was incubated in a 25 °C water bath for 24 h and quenched with 15 μL of stop solution. The product was purified on 12% denaturing PAGE. A typical yield was 20% of the RNA-DNA disulfide conjugate.

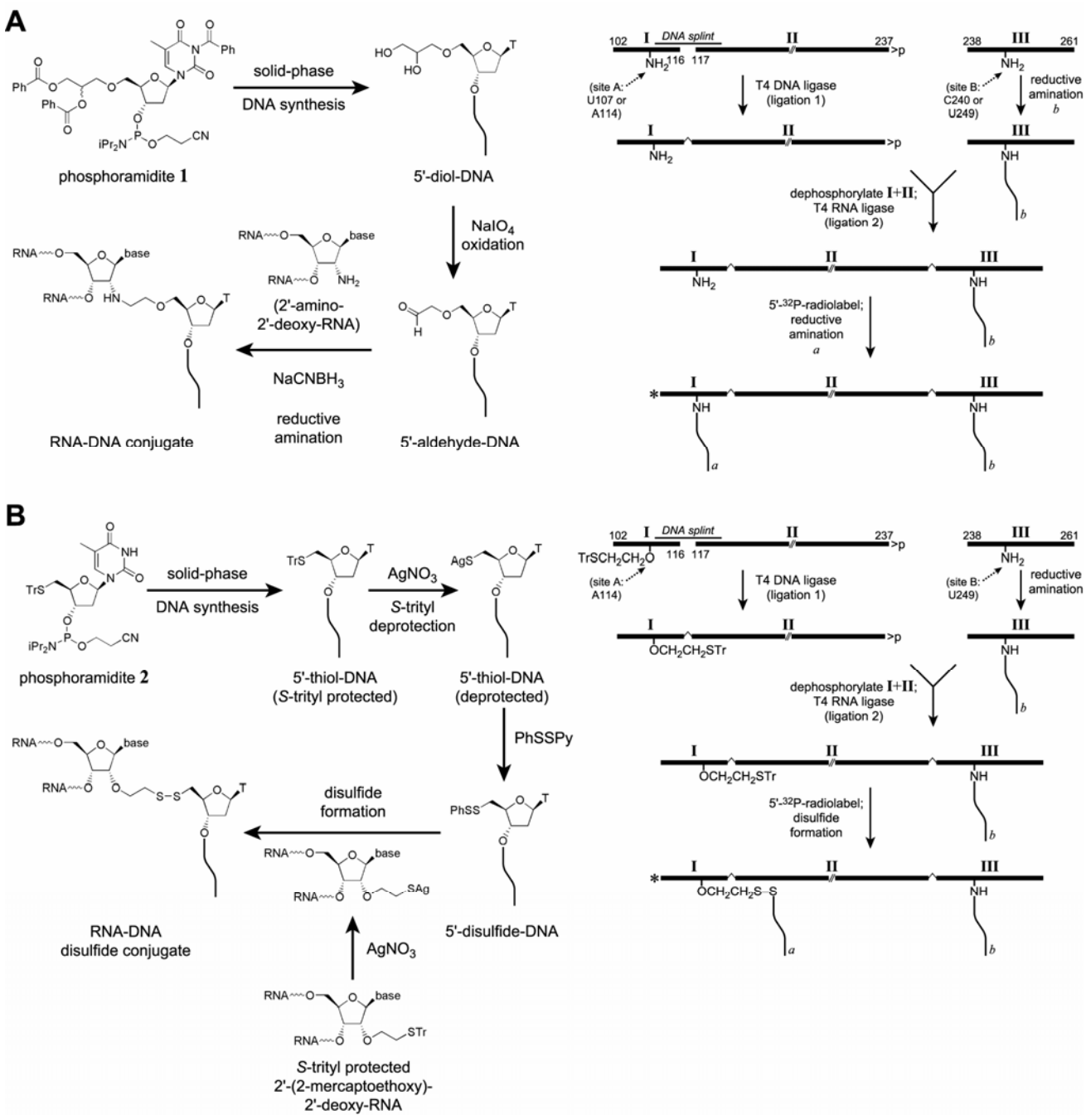


**Figure S2.** Strategies for covalently attaching DNA to RNA. a) *Left*, the chemical reactions for reductive amination, leading to N-linked DNA. *Right*, the strategy to assemble the 160-nucleotide P4-P6 RNA (nucleotides 102-261) with DNA strands attached at two sites by reductive amination. b) *Left*, the chemical reactions for disulfide formation, leading to S-linked DNA. *Right*, the strategy to assemble P4-P6 with one DNA strand attached by disulfide formation.

Experiments with DNA constraints attached at P4-P6 nucleotides A114 and U249

The originally described duplex DNA constraint on P4-P6 folding was either 10 bp or 20 bp in length and attached at P4-P6 nucleotides U107 and C240.[5] For the experiments described in this manuscript, we wished to use DNA constraints that served two additional purposes, which affects the site of constraint attachment. First, for the experiments that use a restriction endonuclease for DNA cleavage (Figure 2), the constraint must be sufficiently long such that the enzyme can recognize the DNA. Because the U107-C240 20-bp constraint had little energetic effect,[5] we used the 20-bp constraint at A114-U249. Second, for the experiments that use a pyrene chromophore to report on RNA folding (Figure 4 and Figure S5), we preferred to use nucleotide U107 as the pyrene attachment site due to our substantial familiarity with P4-P6 labeled at this position.[1,7-9] Both of these considerations suggested that we move the constraint location to nucleotides A114 and U249 in several instances. By using these alternative attachment sites, we have a constraint that affects the P4-P6 RNA structure when the constraint is either 10 bp or 20 bp in length and also leaves U107 available for pyrene derivatization. A comprehensive report of the site- and length-dependence of the DNA constraint effect will be published elsewhere.

Modulation of DNA constraint by addition of nuclease or reducing agent (Figure 2)

*DNA constraint sequences.* The 20-bp DNA constraint was attached at nucleotides A114-U249. For all experiments in Figure 2a except those using BsrBI where the DNA lacked the BsrBI site (– BsrBI), the sequences were 5′-TGGAGAGCGGTGGACGGCGA-3′ and 5′-TCGCCGTCCACCGCTCTCCA-3′ (attached at A114 and U249, respectively). The BsrBI site is underlined, although this is irrelevant for the experiments in which a nonspecific nuclease (DNase or ExoIII) was used. For the – BsrBI experiments, the sequences were 5′-TCGGGAGGCTGGGAAGGGCA-3′ and 5′-TGCCCTTCCCAGCCTCCCGA-3′ (attached at A114 and U249, respectively). Each 5′-T was modified as shown in Figure S2a except for the experiments of Figure 2b in which an S-linked constraint was used, where the 5′-T was modified as shown in Figure S2b.

*Constraint modulation by addition of DNase or Exonuclease III (Figure 2a).* The 5′-$^{32}$P-radiolabeled RNA (~50 fmol) was mixed with 10 pmol of carrier RNA (sequence $A_{13}$) in a total volume of 3 μL containing 5 mM Tris (pH 7.5), 50 mM NaCl, and 0.1 mM EDTA. The sample was annealed by heating at 95 °C for 3 min and cooling on ice for 5 min. For DNase, the sample was brought to 6 μL total volume containing 40 mM Tris (pH 8.0), 1 mM $CaCl_2$, 2 mM $MgCl_2$, 10 U RNase inhibitor (Roche), and 1 U RQ1 DNase (Promega). For ExoIII, the sample was brought to 6 μL total volume containing 10 mM bis-tris propane-HCl (pH 7.0), 2 mM $MgCl_2$, 1 mM DTT, 10 U RNase inhibitor (Roche), and 100 U ExoIII (New England Biolabs). For both DNase and ExoIII, the sample was incubated at 37 °C for 5 h; diluted to 50 μL with water; extracted with 25:24:1 phenol-chloroform-isoamyl alcohol; mixed with 8 μg carrier tRNA, precipitated with ethanol; and dissolved in 10 μL of water. A 2-μL portion of this sample was used for native gel electrophoresis as described.[5] Similar data were obtained (but with occasional smearing of bands) when the phenol-chloroform extraction was omitted and the samples were used directly for native gel electrophoresis as described in the text (data not shown).

*Constraint modulation by addition of BsrBI restriction enzyme (Figure 2a).* The 5′-$^{32}$P-radiolabeled RNA (~50 fmol) was mixed with 10 pmol of carrier RNA (sequence $A_{13}$) in a total volume of 3 μL containing 5 mM Tris (pH 7.5), 50 mM NaCl, and 0.1 mM EDTA. The sample was annealed by heating at 95 °C for 3 min and cooling on ice for 5 min. The sample was brought to 6 μL total volume containing 50 mM Tris (pH 8.0), 2 mM $MgCl_2$, 1 mM DTT, and 10 U BsrBI (New England Biolabs), then incubated at 37 °C for 5 h. The sample was purified and prepared for native gel electrophoresis as described.[5] Similar data were obtained (but with smearing of bands) when the phenol-chloroform extraction was omitted and the samples were used directly for native gel electrophoresis (data not shown).

*Constraint modulation by reduction of a disulfide linkage (Figure 2b).* The 5′-$^{32}$P-radiolabeled RNA (~50 fmol) was mixed with 10 pmol of carrier RNA ($A_n$ oligomer) in a total volume of 3 μL containing 5 mM Tris (pH 7.5), 50 mM NaCl, and 0.1 mM EDTA. The sample was annealed by heating at 95 °C for 3 min and cooling on ice for 5 min. The sample was brought to 5 μL total volume containing 100 mM sodium phosphate (pH 7.5), and 20 mM DTT or 25 mM TCEP, then incubated at 37 °C for 1 h. The sample was prepared for native gel electrophoresis (without purification) as described.[5]

In Figure 2b, which is reproduced below in Figure S3 with inclusion of lane labels 1–4 for reference, the relative mobilities of the foldable (F) and nonfoldable (N) RNAs are observed to change when the constraint is removed by reduction. Specifically, before constraint removal (–), F and N have approximately equal mobilities (lanes 1 and 2 for both DTT and TCEP), whereas after constraint removal (+), F migrates much more quickly than N (lanes 3 and 4). This increase in mobility of F relative to N is characteristic of RNA tertiary folding upon constraint removal. The decreased *absolute* mobility of N after constraint removal (compare lanes 2 and 4) indicates a generic decrease in compactness. For F, this effect is countered by an increase in compactness specifically due to tertiary folding, which leaves the overall absolute mobility of F approximately unchanged (compare lanes 1 and 3). In support of this interpretation, the same absolute mobilities of F and N as in lanes 3 and 4 are observed when a DNA duplex is attached via only the single U249 terminus (data not shown), which provides an essentially equivalent nucleic acid complex to that formed after disulfide reduction.

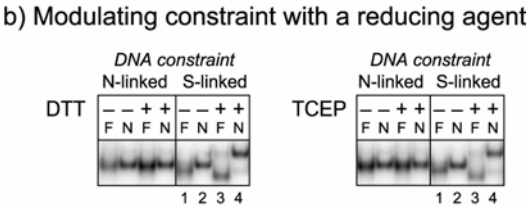


**Figure S3.** Data of Figure 2b, with inclusion of lane labels 1–4 for reference.

*Denaturing PAGE experiments to accompany Figure 2.* From each 10-μL sample described above, 2 μL was mixed with 3 μL of stop solution and loaded into one lane of a 8% denaturing polyacrylamide gel (Figure S4). The results demonstrate that the nucleases or reducing agents cleave the DNA constraint strands as expected, regardless of whether or not the RNA can adopt tertiary structure (i.e., foldable = F or nonfoldable = N).

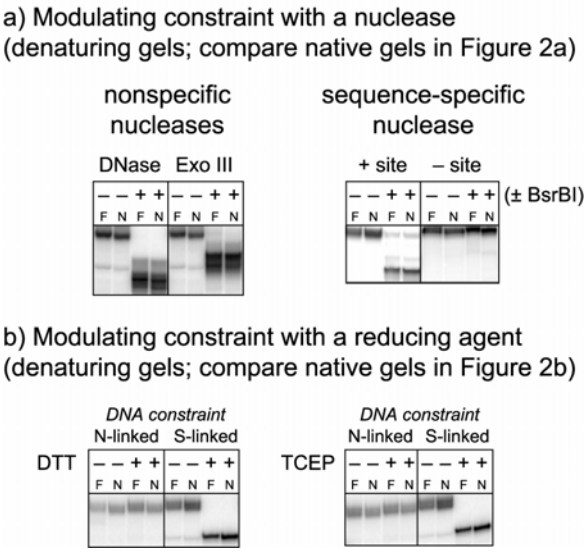


**Figure S4.** Denaturing gel experiments to accompany the native gel data in Figure 2. The data reveal the expected loss of nucleotides due to nuclease cleavage or disulfide reduction for both the foldable (F) and nonfoldable (N) RNA samples.

Modulation of DNA constraint by addition of oligonucleotides (Figure 3a)

The DNA constraint strands were attached at nucleotides U107 and C240; the duplex portion of the constraint was 10 bp in length and the U107 strand had a 10-nt 3′-extension. The native gel electrophoresis protocol described previously[5] was used, except all experiments were performed at 35 °C. The 5′-$^{32}$P-radiolabeled RNA (~50 fmol) was mixed with 10 pmol of carrier RNA (sequence $A_{13}$) in a total volume of 3 μL containing 5 mM Tris (pH 7.5), 50 mM NaCl, and 0.1 mM EDTA. The sample was annealed by heating at 95 °C for 3 min and cooling on ice for 5 min. To the sample was added 3 μL of 2× native gel loading buffer, which contained 2× TB, 10% glycerol, and twice the final desired concentration of 1.5 mM $MgCl_2$ (1× TB contains 89 mM each Tris and boric acid, pH 8.3). The concentration of $MgCl_2$ was adjusted to account for the 0.1 mM EDTA present in the annealing buffer. The sample was annealed by heating at 50 °C for 5 min and cooling at 25 °C for 5–10 min, then 5 μL of the annealed sample was loaded into a gel lane. The gels were electrophoresed at 150–200 V and 25 °C for 5–7 h on 8% polyacrylamide gels containing 7 M urea and 1× TB (made using a 40% 29:1 acrylamide:bis-acrylamide stock solution), then dried and exposed to a PhosphorImager screen. When the complementary (C) strand was employed, 100 pmol was added before the initial annealing step. When the rescue (R) strand was employed, 150 pmol was added and a second annealing step was performed in a total volume of 5 μL. Experiments with the C240 strand instead of the U107 strand extended at its 3′-end gave equivalent results (data not shown). In addition, experiments with a 10-bp constraint at A114-U249 instead of U107-C240 gave equivalent results (data not shown). The sequences of DNA constraint, complement (C) strand, and rescue (R) strand are listed below. Each 5′-T was modified as shown in Figure S2a. In all strands, the nucleotides that compose the intact constraint are boldface and the 10-nt 3′-extension or its complement is underlined; in the C strands, the nucleotides complementary to the 10-nt 3′-extension are underlined; and in the C and R strands, mismatches between the C and original constraint strands are double-underlined.

DNA constraint strand at U107, 5′-**TCGCCGTCCA**CCGCTCTCCA-3′
DNA constraint strand at C240, 5′-**TGGACGGCGA**-3′
C strand with 0 mismatches, 5′-AGGAGAGCGGGTGGTATGGGCAGGTGAAGGTGGAGAGCGG**TGGACGGCGA**-3′
C strand with 2 mismatches, 5′-AGGAGAGCGGGTGGTATGGGCAGGTGAAGGTGGTGAGAGG**TGGACGGCGA**-3′
C strand with 4 mismatches, 5′-AGGAGAGCGGGTGGTATGGGCAGGTGAAGGTCGTGACCCG**TGGACGGCGA**-3′
R strand for C with 0 mismatches, 5′-CCGCTCTCCACCTTCACCTGCCCATACCACCCGCTCTCCT-3′
R strand for C with 2 mismatches, 5′-CC**T**CTC**A**CCACCTTCACCTGCCCATACCACCCGCTCTCCT-3′
R strand for C with 4 mismatches, 5′-C**G**G**G**TC**A**C**G**ACCTTCACCTGCCCATACCACCCGCTCTCCT-3′

Detection of DNA constraint modulation using pyrene fluorescence (Figure 3b)

A P4-P6 RNA was prepared that was both pyrene-labeled and DNA-constrained. The pyrene was covalently attached at P4-P6 nucleotide U107 via a short tether (pyr3) as described.[1,7] The DNA constraint was the A114-U249 10-bp constraint. The DNA strand that is attached via A114 included a 10-nt 3′-extension as described above for U107 (the sequences used here at A114/U249 were the same as used above for U107/C240). Synthetic access to the pyrene-labeled and DNA-constrained RNA used the general procedure described in Figure S2, where oligoribonucleotide **I** had pyrene tethered at U107 as well as a 2′-amino group at A114. In the experiment of Figure 3b, 100 pmol of pyrene-labeled RNA was annealed in 660 μL of 1× TB and 2 mM $MgCl_2$ by heating at 50 °C for 5 min and cooling at 35 °C for 5 min. Into a fluorescence cuvette was placed 650 μL of this solution, and the fluorescence emission spectrum was recorded at 35 °C [1,7]. Sequential 3-μL portions of oligonucleotide C (500 pmol) or R (with 4 mismatches; 600 pmol) in 1× TB and 2 mM $MgCl_2$ were added. After each addition, the sample was equilibrated at 35 °C for 1 h; the fluorescence emission spectrum was recorded and corrected for the slight dilution. The emission intensity at 380 nm was used to obtain the data for the Figure 3b inset.

Fluorescence titration of pyrene-labeled DNA-constrained RNA with $Mg^{2+}$

The pyrene fluorescence data were additionally used to provide independent evidence of $Mg^{2+}$-induced tertiary folding for the DNA-constrained P4-P6. This was achieved by titrating the above pyrene-labeled DNA-constrained P4-P6 with $MgCl_2$ (Figure S5) using previously described protocols.[1,7,8] The data revealed a large RNA tertiary folding component at the $Mg^{2+}$ midpoint ($[Mg^{2+}]_{1/2}$ value, ~8 mM) that was expected on the basis of the native gel experiments shown in Figure 2 of ref. 5. The presence of the second higher-$Mg^{2+}$ component (which is not due to tertiary folding) is also consistent with our previous observations for pyrene-labeled P4-P6 [1,7,8]. The fluorescence experiments allow us to increase the $Mg^{2+}$ concentration much higher than in the native gel electrophoresis experiments (400 mM versus 20 mM), and therefore we can observe a greater portion of the titration curve. The native gel experiments cannot be performed at $Mg^{2+}$ concentrations much greater than 20 mM due to physical limitations inherent to electrophoresis.

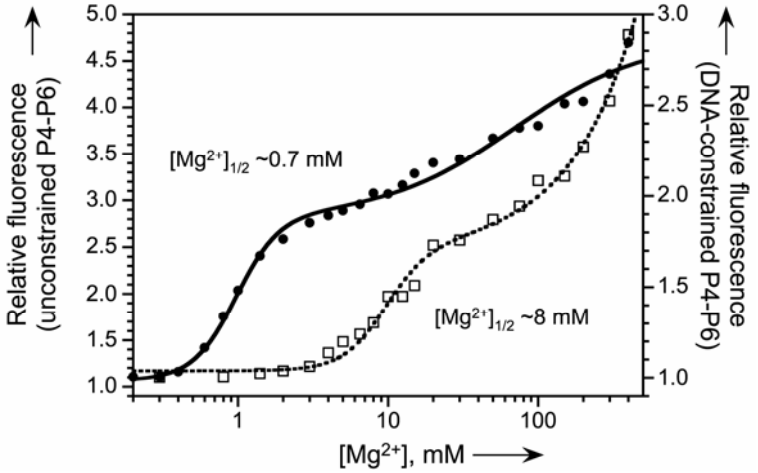


**Figure S5**. Equilibrium fluorescence titration with $Mg^{2+}$ of pyrene-labeled DNA-constrained P4-P6 (pyrene at U107 and 10-bp DNA constraint at A114-U249; *open squares*). The $[Mg^{2+}]_{1/2}$ value for the lower-$Mg^{2+}$ component of ~8 mM is consistent with the native PAGE data in Figure 2 of ref. 5. For comparison, analogous titration data for pyrene-labeled unconstrained P4-P6 is shown (*filled circles*).

Modulation of DNA constraint by formation of ligand-aptamer interactions (Figure 4)

The DNA constraint was a 10-bp duplex attached at P4-P6 nucleotides A114 and U249. The DNA strand attached at A114 incorporated the 18-nt hemin aptamer sequence[10] as follows: 5′-**TGGTGGGTAG**GGCGGGTTGG-3′. The constraint is boldface; the aptamer sequence is underlined; the nucleotide changed in the G9A aptamer mutant[11] is double-underlined. The DNA strand attached at U249 comprised the complementary portion of the constraint as follows: 5′-**TCTACCCACCA**-3′. In the native PAGE experiments, the gels, running buffer, and loaded samples were each prepared using 1× TB buffer with $MgCl_2$[5] and additionally with 1 μM hemin and 20 mM KCl if appropriate. No constraint modulation was observed when hemin was included in the absence of KCl (data not shown).

We explain the effect of hemin on the DNA-constrained RNA folding as follows (see Figure S6):

(*i*) The general model for $Mg^{2+}$-dependent P4-P6 RNA folding is that the unfolded RNA state (U) binds *n* $Mg^{2+}$ ions to form the folded RNA state (F), according to $U + nMg^{2+} \leftrightarrows F \bullet nMg^{2+}$ (equation 1 of Figure S6). As described,[12] the observed native PAGE mobility is a weighted average of the mobilities of the U and F states of the RNA, due to fast equilibration on the hours timescale of the gel experiment. The folding $\Delta G°'$ is related to the $Mg^{2+}$ dependence of RNA folding according to the equation $\Delta G°' = +nRT \bullet \ln[Mg^{2+}]_{1/2}$, where $[Mg^{2+}]_{1/2}$ is the $Mg^{2+}$ midpoint of the curve obtained by plotting relative mobility against $[Mg^{2+}]$. The relative mobility is calculated with reference to the mobility of a nonfoldable mutant version of the RNA as described previously.[5,12]

(*ii*) Covalent attachment of a duplex DNA constraint at A114-U249 is energetically neutral with respect to the unfolded RNA because the duplex is presumed to be structurally compatible with the unfolded state. In contrast, attachment of the DNA duplex at A114-U249 is destabilizing with respect to the folded RNA (equation 2a and possibly 2b). Molecular modeling suggests that all DNA constraints investigated here require only partial melting (equation 2a) to allow RNA folding (data not shown).[5] Therefore, the $[Mg^{2+}]_{1/2}$ value for the duplex-modified P4-P6 is shifted to the right relative to wild-type P4-P6, with $\Delta\Delta G^{\circ\prime} = +n\mathrm{RTln}([Mg^{2+}]_{1/2,\mathrm{mod}}/[Mg^{2+}]_{1/2,\mathrm{wt}})$.

(*iii*) Finally, interactions between the ligand (hemin) and the aptamer counteract the destabilization due to the duplex constraint by providing a favorable $\Delta G^{\circ\prime}$ contribution to the overall equilibrium (equation 3). This should shift the $[Mg^{2+}]_{1/2}$ value to the left.

In free solution, the $K_d$ for binding of hemin to its aptamer is ~30 nM.[13] In principle, a plot of $[Mg^{2+}]_{1/2}$ versus [hemin] would allow determination of the $[\mathrm{hemin}]_{1/2}$ value for modulating the DNA constraint. However, in practice such comprehensive data would be very time-consuming to obtain, because a complete set of 10–20 individual native gels *at each hemin concentration* would be required to determine $[Mg^{2+}]_{1/2}$ for each of the ~10 hemin concentrations necessary to obtain an acceptable $[Mg^{2+}]_{1/2}$ versus [hemin] curve (i.e., 100–200 gels in total). As an alternative, we obtained an order-of-magnitude estimate of $[\mathrm{hemin}]_{1/2}$ by examining the modulation of the DNA constraint at fixed $[Mg^{2+}]$ = 1.5 mM and [hemin] of either 0.2, 0.5, 1.0, and 2.0 μM (the data in Figure 4 were obtained at 1.0 μM hemin). Using 0.2 μM hemin led to almost no constraint modulation; 0.5 μM hemin led to measurable but decreased constraint modulation relative to 1 μM hemin; and 2 μM hemin had essentially the same effect as 1 μM hemin. From these data (not shown), we estimate the $[\mathrm{hemin}]_{1/2}$ as ~0.5–1 μM.

Why is the $[\mathrm{hemin}]_{1/2}$ value different than $K_d$? The basic design principle of the DNA constraint experiment (as implemented in Figure 4) is that RNA folding (equation 1 of Figure S6) cannot occur unless the DNA constraint is disrupted (equation 2). However, to allow RNA folding the DNA constraint does not necessarily have to be disrupted completely (equations 2a + 2b). The disruption could instead be partial yet still permit U → F to occur (equation 2a only; single-stranded DNA can extend to much greater length than an equivalent number of nucleotides that are restricted to duplex conformation). If RNA folding were to require complete disruption of the DNA constraint (equations 2a + 2b), then ligand-aptamer interactions (equation 3) should be observed via their effect on the modulating the DNA constraint with $[\mathrm{hemin}]_{1/2} = K_d$. In contrast, if RNA folding requires only partial disruption of the DNA constraint (equation 2a only), then ligand-aptamer interactions incur an additional $\Delta G^{\circ\prime}$ penalty that corresponds to the $\Delta G^{\circ\prime}$ for completing disruption of the DNA duplex (equation 2b). Others have observed analogous rightward shifts in "apparent $K_d$ values" for ligand-aptamer interactions when coupled with other equilibria.[14]

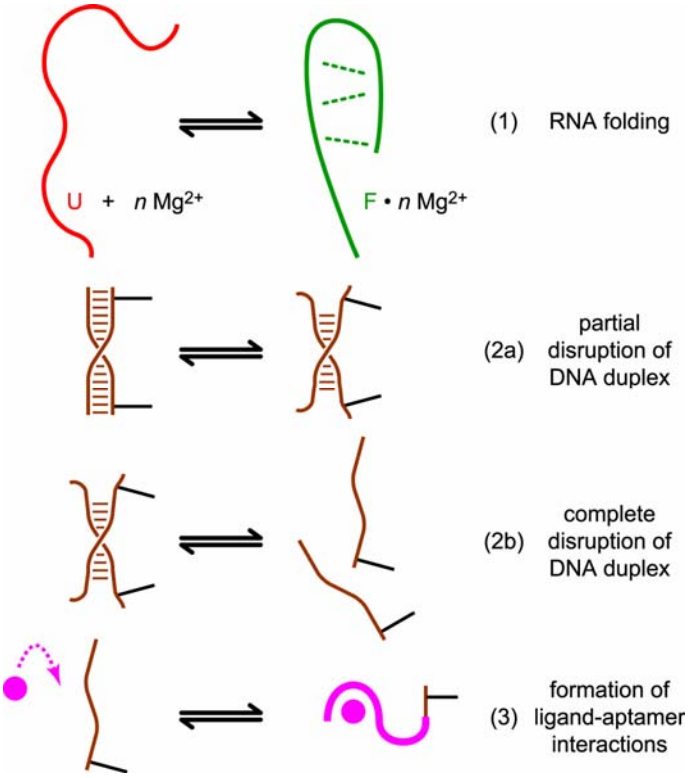


**Figure S6**. Individual equilibria of the RNA folding experiment that involves a DNA constraint and ligand-aptamer interactions. See Figure 4 for an image that places all components within one set of structures.

## References for Supporting Information

[1] S. K. Silverman, T. R. Cech, *Biochemistry* **1999**, *38*, 14224-14237.
[2] a) F. L. Murphy, T. R. Cech, *Biochemistry* **1993**, *32*, 5291-5300; b) A. A. Szewczak, T. R. Cech, *RNA* **1997**, *3*, 838-849.
[3] B. L. Golden, A. R. Gooding, E. R. Podell, T. R. Cech, *RNA* **1996**, *2*, 1295-1305.
[4] a) A. Flynn-Charlebois, Y. Wang, T. K. Prior, I. Rashid, K. A. Hoadley, R. L. Coppins, A. C. Wolf, S. K. Silverman, *J. Am. Chem. Soc.* **2003**, *125*, 2444-2454; b) Y. Wang, S. K. Silverman, *Biochemistry* **2003**, *42*, 15252-15263.
[5] C. V. Miduturu, S. K. Silverman, *J. Am. Chem. Soc.* **2005**, *127*, 10144-10145.
[6] M. Mag, S. Luking, J. W. Engels, *Nucleic Acids Res.* **1991**, *19*, 1437-1441.
[7] B. T. Young, S. K. Silverman, *Biochemistry* **2002**, *41*, 12271-12276.
[8] M. K. Smalley, S. K. Silverman, **2005**, submitted for publication.
[9] a) S. K. Silverman, M. Zheng, M. Wu, I. Tinoco, Jr., T. R. Cech, *RNA* **1999**, *5*, 1665-1674; b) S. K. Silverman, M. L. Deras, S. A. Woodson, S. A. Scaringe, T. R. Cech, *Biochemistry* **2000**, *39*, 12465-12475; c) S. K. Silverman, T. R. Cech, *RNA* **2001**, *7*, 161-166.
[10] a) Y. Li, C. R. Geyer, D. Sen, *Biochemistry* **1996**, *35*, 6911-6922; b) P. Travascio, Y. Li, D. Sen, *Chem. Biol.* **1998**, *5*, 505-517.
[11] H.-W. Lee, D. J.-F. Chinnapen, D. Sen, *Pure Appl. Chem.* **2004**, *76*, 1537-1545.
[12] S. K. Silverman, T. R. Cech, *Biochemistry* **1999**, *38*, 8691-8702.
[13] P. Travascio, A. J. Bennet, D. Y. Wang, D. Sen, *Chem. Biol.* **1999**, *6*, 779-787.
[14] a) R. Nutiu, Y. Li, *J. Am. Chem. Soc.* **2003**, *125*, 4771-4778; b) R. Nutiu, Y. Li, *Chem. Eur. J.* **2004**, *10*, 1868-1876.